

 Open access • Journal Article • DOI:10.1109/TAP.2011.2163761

## **Design of an Implantable Slot Dipole Conformal Flexible Antenna for Biomedical Applications** — [Source link](#)

Maria Lucia Scarpello, Divya Kurup, Hendrik Rogier, D. Vande Ginste ...+5 more authors

**Institutions:** Ghent University, Intec, Inc.

**Published on:** 04 Aug 2011 - IEEE Transactions on Antennas and Propagation (IEEE)

**Topics:** Coaxial antenna, Loop antenna, Antenna measurement, Monopole antenna and Slot antenna

Related papers:

- [Design of a Dual-Band Implantable Antenna and Development of Skin Mimicking Gels for Continuous Glucose Monitoring](#)
- [Implanted antennas inside a human body: simulations, designs, and characterizations](#)
- [Design of implantable microstrip antenna for communication with medical implants](#)
- [Performances of an Implanted Cavity Slot Antenna Embedded in the Human Arm](#)
- [Guidelines for limiting exposure to time-varying electric, magnetic, and electromagnetic fields \(up to 300 GHz\)](#)

Share this paper:    

View more about this paper here: <https://typeset.io/papers/design-of-an-implantable-slot-dipole-conformal-flexible-5fyrnxufh3>

# Design of an Implantable Slot Dipole Conformal Flexible Antenna for Biomedical Applications

Maria Lucia Scarpello<sup>1</sup>, Divya Kurup<sup>2</sup>, Hendrik Rogier<sup>1</sup>, *Senior Member, IEEE*,

Dries Vande Ginste<sup>1</sup>, *Member, IEEE*, Fabrice Axisa<sup>3</sup>, Jan Vanfleteren<sup>3</sup>, *Member, IEEE*, Wout

Joseph<sup>2</sup>, *Member, IEEE*, Luc Martens<sup>2</sup>, *Member, IEEE*, Gunter Vermeeren<sup>2</sup>

<sup>1</sup> Ghent University, Department of Information Technology (INTEC), Electromagnetics Group, Sint-Pietersnieuwstraat 41, B-9000 Gent, Belgium.

e-mail: marialucia.scarpello@ugent.be.

<sup>2</sup> Ghent University, Department of Information Technology (INTEC), UGent-WiCa, Complex Zuiderpoort Blok C0 bus 201 Gaston Crommenlaan 8, B-9050 Gent, Belgium.

<sup>3</sup> Ghent University, ELINTEC-TFCG, Technologiemark 914 B-9052 Gent, Belgium.

**Abstract**—We present a flexible folded slot dipole implantable antenna operating in the Industrial, Scientific, and Medical (ISM) band (2.4–2.4835 GHz) for biomedical applications. To make the designed antenna suitable for implantation, it is embedded in biocompatible Polydimethylsiloxane (PDMS). The antenna was tested by immersing it in a phantom liquid, imitating the electrical properties of the human muscle tissue. A study of the sensitivity of the antenna performance as a function of the dielectric parameters of the environment in which it is immersed was performed. Simulations and measurements in planar and bent state demonstrate that the antenna covers the complete ISM band. In addition, Specific Absorption Rate (SAR) measurements indicate that the antenna meets the required safety regulations.

**Index Terms**—Implantable antennas, Industrial, Scientific and Medical (ISM) band, Specific Absorption Rate (SAR), bent antenna, muscle tissue sensitivity.

## I. INTRODUCTION

Implantable devices are becoming widely researched for different fields of applications, both for humans and animals. Some examples of applications are: monitoring blood pressure and temperature, tracking dependent people or lost pets, wirelessly transferring diagnostic information from an electronic device implanted in the human body for human care and safety, such as a pacemaker, to an external RF receiver [1]. Small implantable biomedical devices placed inside the human body may improve the lives of numerous patients. Patients with the antenna implanted in the body regularly return to the hospital for checkups, where their status and the status of the implant are verified. With the use of RF technology, data recorded by the implanted antenna can be transmitted wirelessly to the receiving station, while the patient is waiting in the lounge. Some patients may require checks every day. In such case a home care unit can be placed in the patient's home. The unit can communicate with the medical implant and can be connected to the telephone system, or the internet, and send data regularly to the responsible person at the hospital [2].

The state-of-the-art of research in implantable antennas

shows that microstrip or planar-inverted F antennas (PIFA), operating in the 402–405 MHz Medical Implant Communications Service (MICS) band, were simulated [3] and also fabricated and measured [4]–[6]. The main issue with this kind of antennas, operating at 403 MHz and thus corresponding to a wavelength of 744.4 mm in free space, is that it is not practical to put them into a living human body without performing thorough miniaturization. Indeed, taking the effect of the body into account during the design, reducing the antenna size by around seven times, without miniaturization it still remains too big to be implanted. In [5], the designed antenna has a cylinder height of 22.72 mm and an external radius of 10.5 mm, and so it is a small size antenna. However, the reflection coefficient value shown in the paper is only simulated and not measured and the simulated MICS bandwidth is only partially covered. In [6], the designed PIFA antenna is also small, i.e. 22.5 mm × 18.5 mm × 1.9 mm, but its fractional bandwidth is 20% lower than the one of the antenna we propose and it is not embedded in any insulating biocompatible material during measurements. Choosing a higher resonance frequency, corresponding to the Industrial, Scientific, and Medical (ISM) band (2.4–2.4835 GHz), is one way to reduce the antenna size and making it available to be implanted. Another advantage has to do with the radio communication link: the larger bandwidth allows for higher bitrates. Implantable H-shaped slot cavity antennas are studied for 2.45 GHz applications in [7], [8]. In [7], the antenna was simulated, whereas in [8] the same antenna was reduced in size. But since the size was too small to be fabricated (2.8 mm × 4.0 mm × 1.6 mm), the antenna was rescaled to larger dimensions to be manufactured and measured in order to be able to compare measurements with the finite-difference time-domain (FDTD) simulations. Radiation patterns, gain pattern, and radiation efficiency value are related to the rescaled antenna and to a rescaled resonance frequency equal to 980 MHz. Moreover in [8], no biocompatible material was used to embed the antenna and the cable during the measurements. In [9], [10], two dual band implantable antennas are presented, working properly in the MICS band and in the ISM band. Measurements

were performed in a human skin mimicking gel tissue and in a rat skin mimicking gel tissue, respectively. In [10], the gain pattern is simulated and its maximum value is  $-10$  dBi in the ISM band. However, the two antennas are not embedded in any biocompatible material and they are not flexible. In [11] a cardiovascular stent, working at 2.4 GHz has been designed, fabricated, and implanted in a live porcine subject. The stents are left without any insulation material and they are in direct contact with the tissue. In [12] three different inhomogeneous digital phantoms are considered to check the different radiation performances of wireless implants. Here again only simulations are performed but no measurements.

In this paper, we present the design, characterization, and measurements of an implantable antenna operating in the 2.45 GHz ISM band, recommended by the European Radiocommunications Committee (ERC) for ultra-low-power active medical implants [13]. The antenna is a flexible slot dipole. To make the antenna suitable for implantation, it is embedded in biocompatible Polydimethylsiloxane (PDMS). The reflection coefficient was simulated and measured in the MSL2450 liquid, provided by Speag (Zurich, Switzerland) [14], mimicking a 100% human muscle tissue, having well-defined dielectric values at 2.45 GHz. To investigate how different human tissues, surrounding the implanted slot dipole, affect its radiation characteristics, a study on the sensitivity of the liquid mimicking the human muscle tissue was performed. Thereto its dielectric nominal values were varied from 50% larger to 50% smaller. These simulations were performed to ensure that the antenna is functioning properly in any type of body environment. The radiation characteristics of the antenna in terms of E-field and gain were simulated by means of FDTD calculations. For the evaluation of performances and safety issues related to implanted antennas, the 10-g and 1-g averaged specific absorption rate (SAR) are measured and compared with the ICNIRP [15] and with the FCC guidelines [16].

First, in Section II, the antenna design and its fabrication are presented. Next, in Section III, the performance in terms of reflection coefficient is reported. Good agreement is demonstrated between the simulated and measured reflection coefficient. In Section IV, the sensitivity of the antenna as a function of the dielectric properties of the muscle tissue is analyzed, verifying that the antenna can be placed close to different kinds of tissue. In Section V, the radiation characteristics of the antenna, including the measured SAR distribution, are shown. In Section VI conclusions are summarized.

## II. BIOCOMPATIBLE FOLDED SLOT DIPOLE ANTENNA DESIGN AND MANUFACTURING PROCESS

The antenna, presented in this paper, is a flexible folded slot dipole embedded in biocompatible PDMS, as folded slot dipole geometries can provide significantly larger bandwidths than patch antennas [17]. The top and frontal view of the antenna are shown in Figs. 1 and 2, respectively. The dimensions of the folded slot dipole antenna are shown in Table I. The antenna is designed

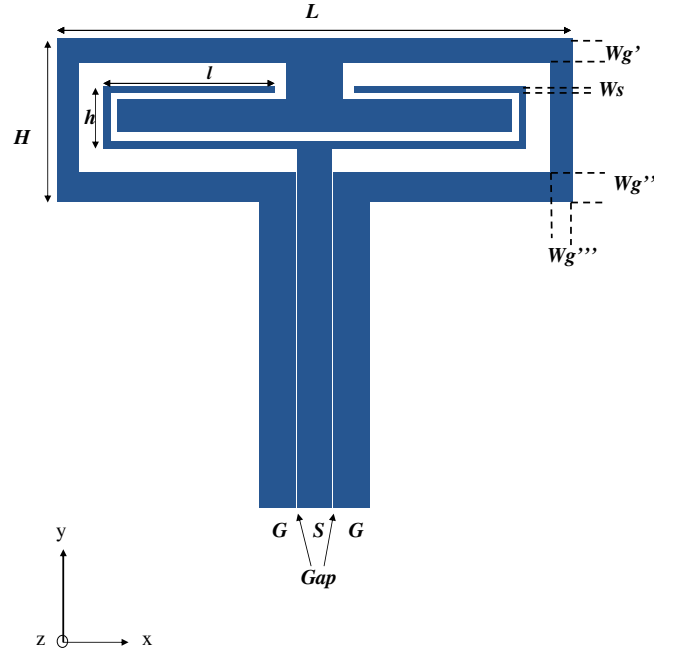


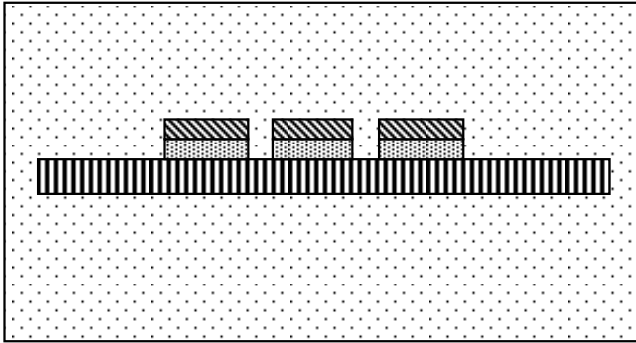
Figure 1: Top view of the coplanar waveguide-fed antenna.

by means of the 2.5-D EM field simulator Momentum of Agilent's Advanced Design System (ADS). The antenna design procedure consists of three steps. First, the folded slot dipole antenna was designed, using ADS's optimization routines, to operate in the 2.45 GHz ISM band in free space. Second, one superstrate and one substrate of PDMS were added to the design and, after the characterization of the PDMS, we redesigned and reoptimized the antenna embedded in silicone so that it covers the ISM band. Third, in a last optimization step, on top of the superstrate and below the substrate one layer of liquid, mimicking the dielectric characteristics of human muscle tissue at 2.45 GHz, was added. Finally, the antenna so designed have good simulations results, working properly in the ISM band. To check more accurately, the antenna was also simulated with the 3-D simulator CST Microwave Studio and the simulation results were still satisfactory. To manufacture the antenna we rely on a flexible electronic technology. A photoresist film was spin-coated on a copper foil and patterned by UV radiation through a photomask; the patterned shape is shown in Fig. 1; two PDMS layers are used as substrate and superstrate, each with a thickness of 2.5 mm, to mould the antenna [18], [19]. The dielectric properties of the PDMS were characterized at 2.45 GHz, to be  $\epsilon_r = 2.2$  and  $\tan \delta = 0.013$ .

The feeding structure of the slot dipole antenna consists

Table I: Size of the folded slot dipole antenna

	[mm]
$H$	8.5
$L$	25.9
$h$	3.2
$l$	8.3
$Wg'$	1.2
$Wg''$	1.5
$Wg'''$	1.0
$Ws$	0.3
$G$	1.8
$S$	1.7
Gap $G-S$	0.1






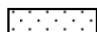
	Copper 9 $\mu\text{m}$
	Nickel 50 nm + Gold 200 nm
	Polyimide 25 $\mu\text{m}$
	PDMS 2.5 mm

Figure 2: Frontal view of the coplanar waveguide-fed antenna.

of a coplanar waveguide (CPW) with a  $50 \Omega$  mode impedance. Matching the mode impedance of the CPW to  $50 \Omega$  is obtained by tuning the distance between the tracks  $G$  and  $S$ , as well as the width of the tracks (Fig. 1). The CPW is fed by a U.FL connector and an ultra-fine Teflon coaxial cable supplied by Hirose [20]. The U.FL connector is chosen (specifically for measurements purposes) because it is compact and it suits the small CPW size. Both the connector and the cable are also embedded in PDMS. Fig. 3 shows the antenna prototype before being embedded in the PDMS. Fig. 4 shows a side view of the antenna prototype with its connector and cable after being embedded in the PDMS.

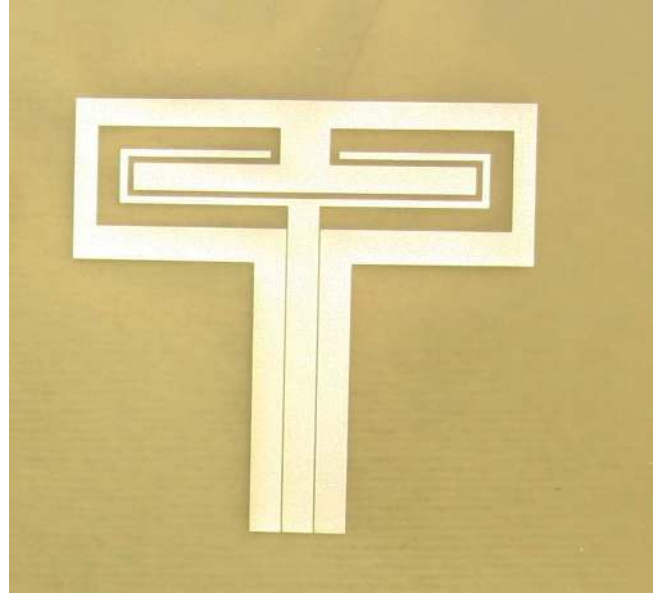


Figure 3: Top view of flex antenna without PDMS.

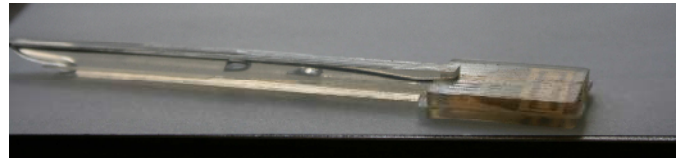


Figure 4: Side view of antenna and cable embedded in PDMS.

### III. SIMULATION AND MEASUREMENTS

In real-life applications, the antenna is intended to be implanted into the human body, subcutaneously, particularly inside the muscle. Hence, the measurement setup, using a phantom, is as follows. The antenna is placed at the center of a plastic container of dimensions  $80 \text{ cm} \times 50 \text{ cm} \times 20 \text{ cm}$  filled with 30 liters of the Human Muscle Tissue liquid MSL2450 [14]. This liquid mimics the dielectric characteristics of human muscle tissue at 2.45 GHz, standardized in [21] to be  $\epsilon_r = 52.7$ ,  $\sigma = 1.73 \text{ S/m}$ ,  $\rho = 1000 \text{ kg/m}^3$ . Dielectric values of the liquid at 2.45 GHz measured by the manufacturer result to be:  $\epsilon_r = 50.8$ ,  $\sigma = 2.01 \text{ S/m}$ ,  $\rho = 1.030 \text{ kg/m}^3$  [14]. In Tables II and III permittivity and conductivity values of the liquid MSL2450 at different frequencies, measured by the manufacturer, and of the human muscle tissue [21], [22], [23] are listed, respectively.

Table II: Dielectric values of MSL2450, at different frequencies.

Frequency [GHz]	$\epsilon_r$	$\sigma \text{ S/m}$
2.0	52.15	1.47
2.4	52.06	1.94
<b>2.45</b>	<b>50.8</b>	<b>2.01</b>
2.5	50.51	2.02
3.0	48.10	2.77

Table III: Dielectric values of human muscle tissue, at different frequencies, as reported in [21], [22], [23].

Frequency [GHz]	$\epsilon_r$	$\sigma$ S/m
2.0	53.29	1.45
2.4	52.79	1.70
<b>2.45</b>	<b>52.72</b>	<b>1.73</b>
2.5	52.66	1.77
3.0	52.05	2.14

The values in Tables II and III cover the band (2.0 GHz and 3.0 GHz) in which the measurements were performed, and as such also encompass the ISM band (2.4-2.485 GHz). Fig. 5 reports the  $S_{11}$  values for each couple of dielectric values reported in Tables II and III, valid at the specified frequency. It can be observed that the small differences in  $\epsilon_r$ ,  $\sigma$ , reported in Tables II and III, do not lead to very different antenna behavior. A third simulation, where a fixed relative permittivity  $\epsilon_r = 50.8$  and a fixed conductivity  $\sigma = 2.01$  S/m were used within the complete band, also indicates that the antenna is rather insensitive to changes of the surrounding medium. This will be further illustrated by considering other human tissues (Figs. 9 and 10). Moreover, a detailed study of the sensitivity of the antenna as a function of the dielectric properties of the liquid is reported in Section IV.

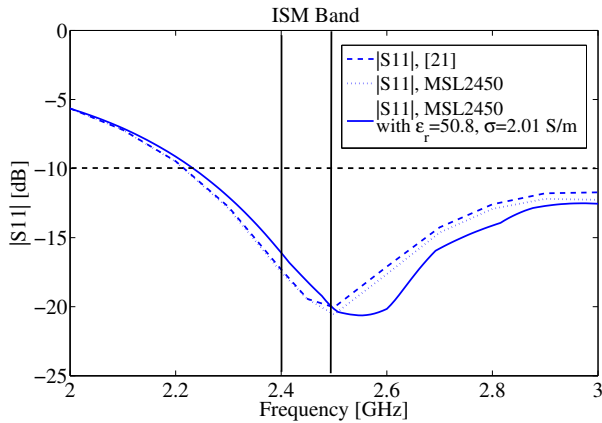


Figure 5:  $S_{11}$  values using the MSL2450 dielectric properties [14] (dotted line) and to human muscle tissue dielectric properties [21] (dashed line), compared to the return loss value of the antenna immersed in a medium with fixed values of permittivity and conductivity, i.e. those of MSL2450 at 2.45 GHz (full line).

The antenna is connected to a Rhode and Schwarz ZVR Network Analyzer, as shown in Figs. 6 and 7. Inside the phantom,  $S_{11}$  measurements are performed when the antenna is both in planar and bent state.

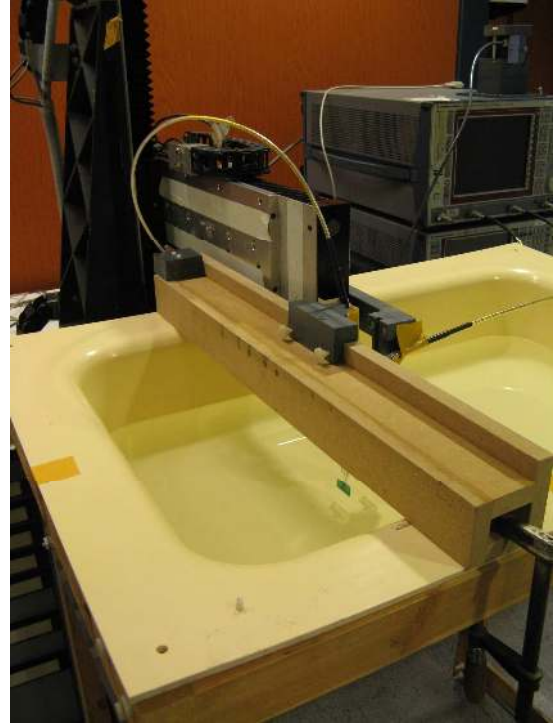


Figure 7: SAR and reflection measurement setup with the implantable antenna inside the liquid during a measurement.

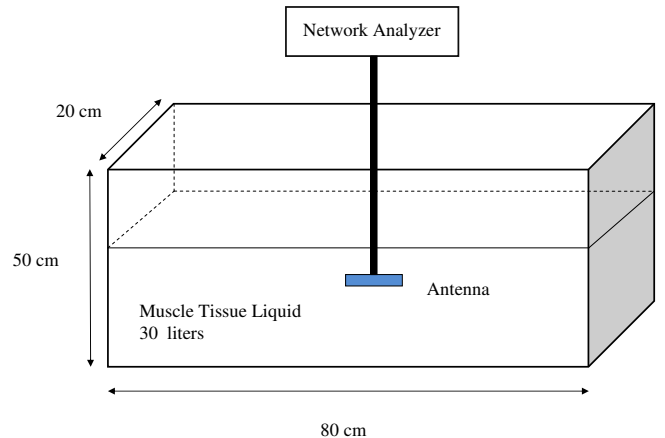


Figure 6: Schematic representation of the reflection measurement setup for the designed implantable antennas using muscle tissue simulating liquid.

First, Fig. 8 displays a comparison between the measured and simulated reflection coefficient of the antenna in planar state. The simulations are performed using the EM field simulator Momentum of Agilent's Advanced Design System

(ADS) and CST Microwave Studio simulator. Since ADS Momentum is a 2.5-D simulator, it does not account for the finite size of the PDMS layers. This finite size typically results in a shift of the resonance frequency to lower frequencies, so for the initial design in Momentum, to cover the ISM band, the antenna is designed to resonate at 2.5 GHz. Once fabricated and measured, this design ensures that our antenna will cover the complete requested bandwidth, as also verified by CST simulations in Fig. 8. The required -10 dB impedance bandwidth of the antenna is 83.5 MHz in the 2.45 GHz ISM band. Simulations and measurements satisfy the requirements: (i) the antenna was simulated in planar state with ADS. Its bandwidth is very wide, 1.23 GHz (2.22-3.45 GHz), it includes different resonances of the antenna and the fractional bandwidth at the target frequency (2.45 GHz) is approximately 50.2%. (ii) The antenna was also simulated in planar state with CST: its bandwidth is 270 MHz (2.30-2.57 GHz) and the fractional bandwidth at the target frequency (2.45 GHz) is approximately 11.0%. (iii) Antenna measurements are performed to validate the simulations: the measured bandwidth in planar state is 350 MHz (2.20-2.55 GHz) and the fractional bandwidth at the target frequency (2.45 GHz) is approximately 14.2%.

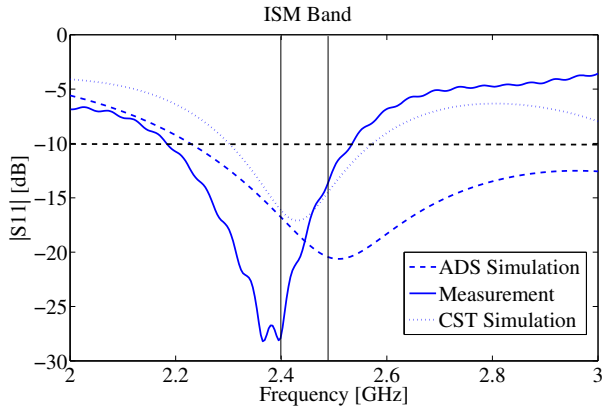


Figure 8: Antenna in planar state: reflection coefficient, simulations vs measurement.

Second, to demonstrate that the antenna can work within different human tissues, the antenna is placed into two human body structures, as reported in [24], [25] and shown in Figs. 9 and 10, and simulated by means of ADS Momentum. The dielectric properties ( $\epsilon_r$ ,  $\sigma$ ), for each layer of the two structures, at  $f = 2.45$  GHz, were obtained from [21], [22] and [23], and shown in Table IV.

Table IV: Dielectric values of four different human tissues, at 2.45 GHz, as reported in [21], [22], [23].

	$\epsilon_r$	$\sigma$ S/m
Muscle	52.72	1.73
Skin	38.00	1.46
Fat	5.28	0.10
Bone	18.54	0.80

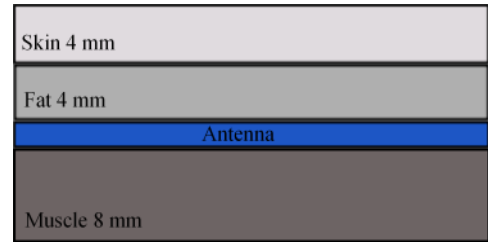


Figure 9: Three layers geometry for the design of the slot dipole antenna, placed in between fat and muscle.

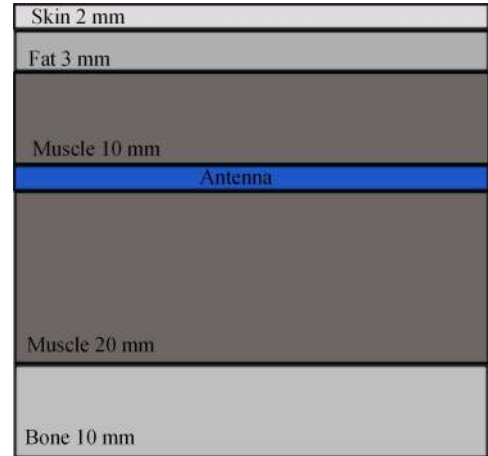


Figure 10: Five layers geometry for the design of the slot dipole antenna, placed in between two layers of muscle.

In Fig. 11, the return loss value of the antenna placed in the structures of Figs. 9 and 10 is shown. A slight shift of the resonance frequency towards higher frequencies can be observed, but the return loss value still remains below -10 dB in the whole ISM band.

Third, the performance of the antenna when it is bent, as such making it conformal to curved parts of the body, is verified. Thereto, the antenna is bent around its x-axis

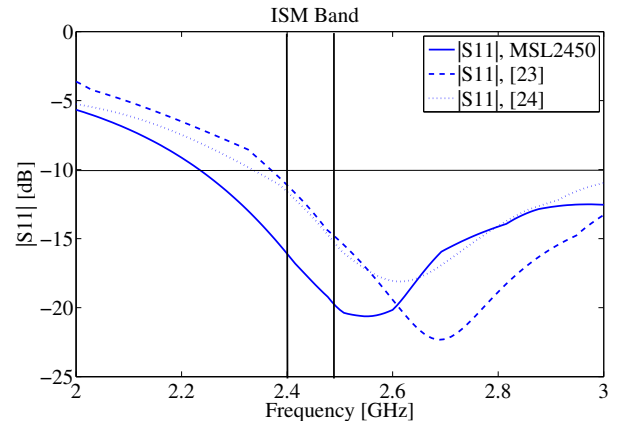


Figure 11: Simulation of the return loss of the antenna placed in the structures of Figs. 9 (dashed line) and 10 (dotted line), compared to the antenna placed in the MSL2450 (full line).



Figure 12: Cylinders used to bend the antenna: 8 cm and 4 cm diameter.

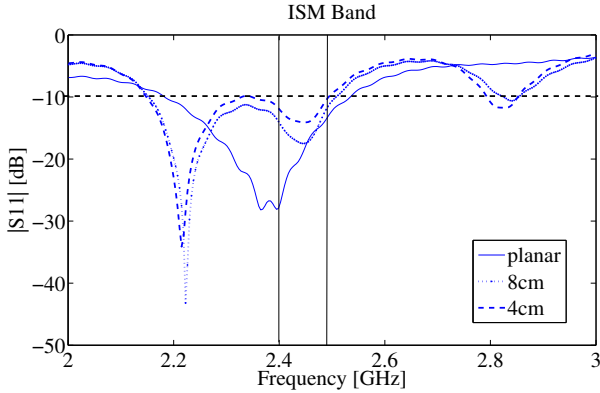


Figure 13: Antenna bent around x-axis vs antenna in planar state: reflection coefficient measurements.

using two cylinders with different diameters, 8 cm and 4 cm, and with a hole in the middle, as shown in Fig. 12. The measured reflection coefficient of the bent antenna is compared to the planar antenna and shown in Fig. 13. The reflection coefficients of the bent antenna exhibits a resonance frequency  $f_r$  at 2.22 GHz. So it is observed that the resonance has shifted to a somewhat lower frequency, compared to  $f_r=2.39$  GHz for the planar antenna. Still, the bandwidth of 350 MHz is maintained and the complete ISM bandwidth is covered.

#### IV. SENSITIVITY OF THE ANTENNA TO DIELECTRIC PROPERTIES OF THE MUSCLE TISSUE

The use of a muscle tissue liquid is widely accepted as a standard, as it is very important to experimentally verify the characteristics of electromagnetic (EM) propagation inside the human body. Muscle tissue exhibits typical anisotropic electric properties [26]: in the low frequency range, the longitudinal conductivity is significantly higher than the transverse conductivity [27]. A variation of conductivity can influence the performance of antennas in real life

applications. Fortunately, the muscle tissue anisotropy is frequency dependent: if the frequency of the current is high enough (i.e., in the MHz range), the anisotropic properties disappear [28]. In this paper, the operation frequency of the antenna is from 2.4 GHz to 2.485 GHz, high enough to neglect the effect of anisotropy. Moreover, the effect of tolerances in the dielectric properties of the different tissues can be significant, potentially influencing communication performance of the implantable slot dipole antenna. Using ADS Momentum, a parametric study is performed that determines the influence of the muscle tissue's permittivity and conductivity on the reflection coefficient of the antenna, in terms of resonance frequency and fractional bandwidth. This is to ensure that the antenna can be implanted at different locations inside the body, also close to tissues having different dielectric characteristics. The electrical properties of the muscle tissue liquid at 2.45 GHz were standardized in [21] to be  $\epsilon_r = 52.7$ ,  $\sigma = 1.95$  S/m,  $\rho = 1000$  kg/m<sup>3</sup>. For the MSL2450 liquid, slightly different values were measured by the manufacturer, resulting in  $\epsilon_r = 50.8$ ,  $\sigma = 2.01$  S/m,  $\rho = 1.030$  kg/m<sup>3</sup> at 2.45 GHz [14]. The dielectric characteristics are now varied as follows:

$$\epsilon_r^{i,j} = \epsilon_r + 0.1 \cdot j \cdot \epsilon_r, \quad \sigma^{i,j} = \sigma + 0.1 \cdot i \cdot \sigma \quad (1)$$

$$i, j = -5, -4, \dots, 4, 5$$

where  $\epsilon_r$  and  $\sigma$  are the nominal values of the liquid, corresponding to the values measured by the manufacturer.

Varying  $\epsilon_r$  and  $\sigma$ , according to (1), results in  $(11)^2 = 121$  simulations. 25 relevant samples are shown in Table V. At the dielectric nominal values, the fractional bandwidth equals 50%, the antenna resonates at 2.51 GHz and  $|S_{11}| = -20.6$  dB. For all the other simulations the fractional bandwidth is always between 48.5% and 51.5%. In the worst case  $|S_{11}| = -16.9$  dB, for  $j = i = 5$ . For all considered variations in dielectric properties, the complete ISM band remains covered and the -10 dB bandwidth results to be very large, showing the lowest frequency equals to 2.2 GHz and the highest one equals to 3.5 GHz. As stated before (Section III), the antenna was designed in ADS-Momentum to resonate at 2.5 GHz to account for a possible shift to lower frequencies due to the finite size of the antenna. As can be seen from the table V, the largest shift can be expected when the relative permittivity of the muscle tissue is drastically lower than its nominal value and when the losses are much higher ( $j = -5$ ,  $i = 5$ ). Still, the shift of the resonance frequency is limited. Therefore, we conclude that the antenna works properly in various human bodies, with considerably different dielectric properties.

#### V. RADIATION CHARACTERISTICS OF THE ANTENNA

Using CST Microwave Studio simulations, the radiation characteristics of the antenna inside the liquid simulating muscle tissue are determined in terms of radiation patterns

Table V: Resonance frequency [GHz] and reflection coefficient [dB] for some couples of  $\epsilon_r$  and  $\sigma$  values.

$\epsilon_r \backslash \sigma$	-50%/1	-20%/1.6	0%/2.01	+20%/2.4	+50%/3
<b>-50%/25.8</b>	2.51	2.48	2.47	2.45	2.44
	-37.2	-56.9	-41.8	-34.7	-29.9
<b>-20%/40.6</b>	2.52	2.51	2.5	2.5	2.48
	-24.8	-24.4	-23.9	-23.3	-22.4
<b>0%/50.8</b>	2.52	2.51	2.51	2.5	2.49
	-20.84	-20.8	-20.6	-20.42	-20
<b>+20%/61.0</b>	2.52	2.51	2.51	2.5	2.5
	-18.85	-18.83	-18.75	-18.65	-18.4
<b>+50%/76.2</b>	2.51	2.51	2.51	2.5	2.5
	-17.18	-17.14	-17.1	-17	-16.9

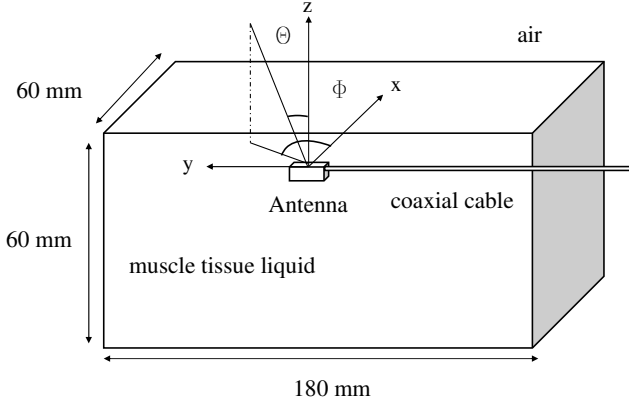
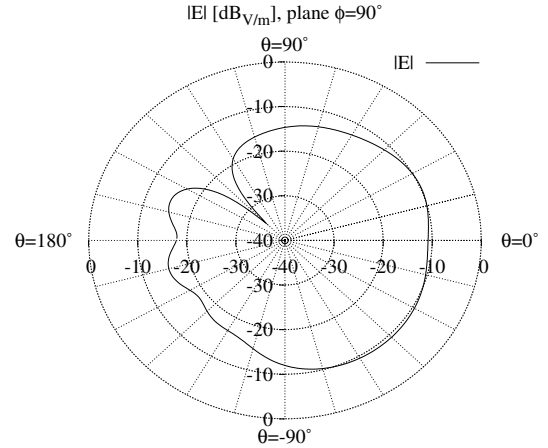
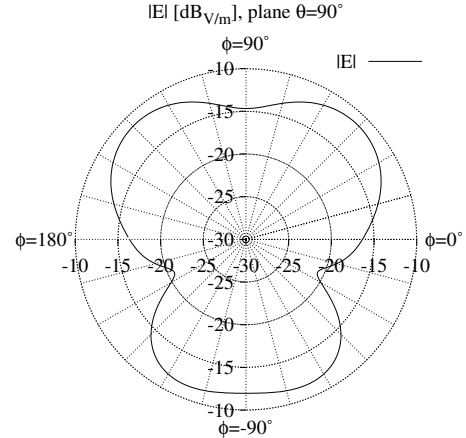


Figure 14: CST numerical calculation model: the box simulates a human arm.

and gain. To simulate, for example, the implanted antenna in the human arm, the dimensions of the box containing the liquid are chosen to be 180 mm x 60 mm x 60 mm, as shown in Fig. 14. The antenna is directed toward the surface of the skin (surface of the box), and along the z-direction the distance to the surface of the skin is set to 4 mm. In the x-y plane, the antenna is placed in the center of the surface of the human model arm (center of the box). This setup is the same as in [8]. The computed radiation patterns in the  $\theta$ -plane ( $\theta = 90^\circ$ ) and the  $\phi$ -plane ( $\phi = 90^\circ$ ) are shown in Figs. 15 and 16. The patterns are computed at 2.45 GHz, at a reference distance of 1 m, and using an input power of 1 W. Fig. 17 shows the antenna gain. The maximum gain is equal to -23.98 dBi for  $\theta = -46^\circ$  and  $\phi = 90^\circ$  and the radiation efficiency is 0.14%. These values are comparable to other results in literature, such as in [8]. The radiation efficiency value is very low because the antenna is not in free space, but embedded inside a human arm, simulated as a very lossy medium.

The SAR is measured in a 3 cm x 3 cm x 2.5 cm cube above the antenna, as reported in Fig. 18. The measurement setup is provided by Speag (Zurich, Switzerland). The measurement system used is DASY 3 [29] and the phantom is filled with the liquid MSL2450 [14]. The size of the box phantom [30] has been chosen to correspond to the average trunk of an adult man. Because sharp edges can cause field modifications, the edges are rounded with a radius of 7 cm. The SAR measurement probe is EX3DV4 [31]. The SAR

Figure 15: Far-field pattern at 2.45 GHz in the  $\theta$ -plane, y-z plane.Figure 16: Far-field pattern at 2.45 GHz in the  $\phi$ -plane, x-y plane.

measurement procedure is described in [32]. Fig. 19 shows the SAR distribution on the x-y plane of the antenna at  $z=0$  when the input power is 2 mW: the peak SAR value is 0.308 W/Kg. The 10-g averaged SAR peak value is 0.032 W/Kg and the 1-g averaged SAR peak value is 0.079 W/Kg. These values fulfill the ICNIRP [15] and FCC [16] guidelines for general public exposure.



## VI. CONCLUSION

The design, manufacturing, measurement, and sensitivity study of a flexible folded slot dipole antenna embedded in PDMS for implantation into the human body was performed. The human body was replaced by a human muscle tissue liquid with known dielectric nominal values. The main issues addressed in this paper are:

- 1) design of a slot dipole antenna suited for implantation into the human body;
- 2) evaluation of the characteristics of the antenna in terms of reflection coefficient in planar and bent state, E-field and gain;
- 3) study of the sensitivity of the liquid mimicking the human muscle tissue, varying its nominal dielectric values;
- 4) checking the SAR limitations, by means of SAR measurements.

Measurements and simulations of the reflection coefficient in planar and bent state in the 2.45 GHz ISM band demonstrate a very large bandwidth in both states, fully covering the ISM band. A good agreement is found between simulations and measurements for the planar state antenna. In bent state, a shift of the resonance towards lower frequencies is verified during measurements. The simulated far-field pattern and gain at 2.45 GHz show a -23.98 dBi gain at  $\theta = -46^\circ$  and  $\phi = 90^\circ$ . The study of the sensitivity with respect to the dielectric properties of surrounding tissue shows that the EM characteristics of the antenna are stable for a wide range of tissue properties in the neighborhood of the antenna. In fact, only for extreme changes of the dielectric properties, the resonance frequency starts shifting. The measured SAR values with an input power of 2 mW averaged in 1-g and 10-g tissue show that the antenna respects the ICNIRP and FCC guidelines for general public exposure. In the future, integration of the required transceiver and power supply is envisaged to realize an implantable system for biotelemetry applications, completely embedded in biocompatible silicone and fabricated with a flexible technology, as shown in [18], [19] by one of the coauthors of this paper. At the current level of our on-going research project, no specific active electronics have yet been developed. The antenna presented in this paper might be slightly large for an immediate implant but it is an important contribution to implantable systems because it is flexible, conformal and completely embedded in biocompatible silicone. It is, important to first simulate and measure a good antenna structure, such as the one presented in this paper, usable as an innovative starting point for future miniaturized design.

## REFERENCES

- [1] B. M. Steinhaus, R. E. Smith, and P. Crosby, "The role of telecommunications in future implantable device systems", *Proc. 16th IEEE EMBS Conf.*, Baltimore, MD, USA, 1994, pp. 1013-1014.

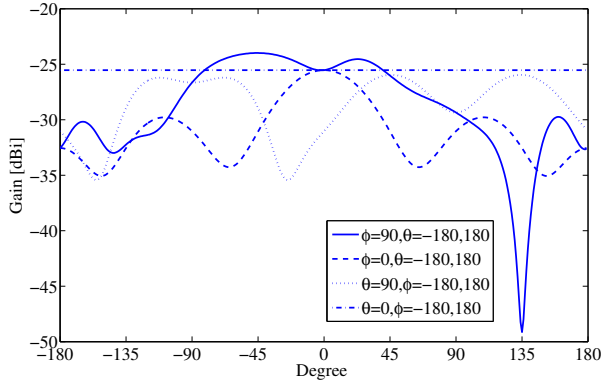


Figure 17: Gain pattern at 2.45 GHz.

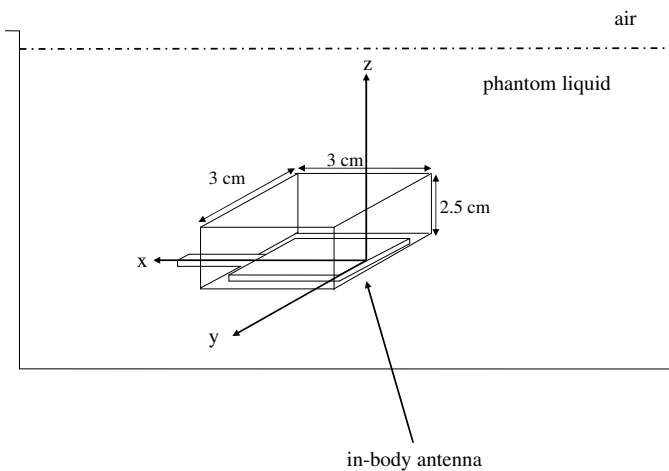


Figure 18: Setup for SAR measurements.

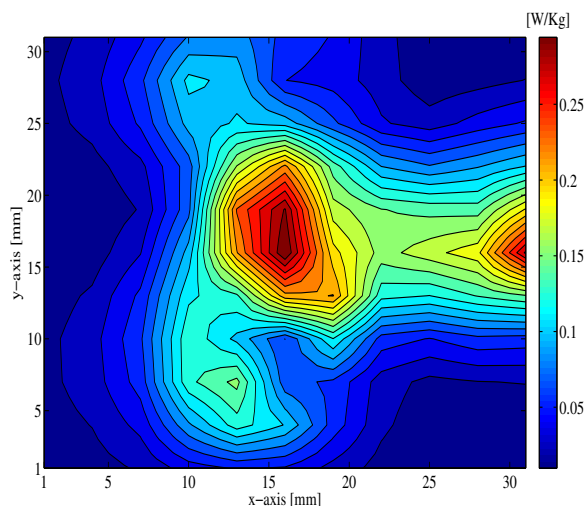


Figure 19: SAR distribution for an input power of 2 mW.

- [2] R. F. Weir, P. R. Troyk, G. De Michele, and T. Kuiken, "Implantable Myoelectric sensors (IMES) for upper-extremity prosthesis control", *Proc. IEEE Eng. Med. Biol. Soc 25th Annu. Int. Conf.*, 2003, pp. 1562-1565.
- [3] K. Y. Yazdandoost, R. Kohno, "An Antenna for Medical Implant Communications System", *IEEE Antennas and Wireless Propagation Letters*, 2007, vol. 6, pp. 392-395.
- [4] J. A. Von Arx, W. R. Mass, S. T. Mazar, and M. D. Amundson, "Antenna for an Implantable Medic Device", U.S. Patent 6708065, Mar. 16, 2004.
- [5] F. Merli, L. Bolomey, E. Meurville, and A. K. Skrivervik, "Implantable Antenna for Biomedical Applications", *IEEE Antennas and Propagation Soc. Int. Symp.* San Diego, CA, USA, 2008, pp. 584-587.
- [6] C. M. Lee, T. C. Yo, F. J. Huang, C. H. Luo, "Bandwidth Enhancement of Planar Inverted-F Antenna for Implantable Biotelemetry", *Microwave and Opt. Tech. Lett.*, Mar. 2009, vol. 51, n. 3, pp. 749-751.
- [7] H. Usui, M. Takahashi, and K. Ito, "Radiation characteristics of an implanted cavity slot antenna into the human body", *Proc. IEEE Antennas and Propagation Soc. Int. Symp.*, Albuquerque, NM, USA, 2006, pp. 1095-1098.
- [8] W. Xia, K. Saito, M. Takahashi, and K. Ito, "Performances of an implanted cavity slot antenna embedded in the human arm", *IEEE Transactions on Antennas and Propagation*, Apr. 2009, vol. 57, n. 4, pp. 894-899.
- [9] T. Karacolak, A. Z. Hood and E. Topsakal, "Design of a Dual-Band Implantable Antenna and Development of Skin Mimicking Gels for Continuous Glucose Monitoring", *IEEE Transactions on Microwave Theory and Techniques*, Apr. 2008, vol. 56, n. 4, pp. 1001-1008.
- [10] T. Karacolak, E. Topsakal, "Electrical Properties of Nude Rat Skin and Design of Implantable antennas for Wireless Data Telemetry", *2008 IEEE MTT-S International Microwave Symp. Digest*, Atlanta, GA, USA, 2008, vol. 1-4, pp. 1169-1172.
- [11] E. Y. Chow, Y. Ouyang, B. Beier, W. J. Chappell, and P. P. Irazoqui, "Evaluation of Cardiovascular Stents as Antennas for Implantable Wireless Applications", *IEEE Transactions on Microwave Theory and Techniques*, Oct. 2009, vol. 57, n. 10, pp. 2523-2532.
- [12] A. Sani, A. Alomainy, and Y. Hao, "Numerical Characterization and Link Budget Evaluation of Wireless Implants Considering Different Digital Human Phantoms", *IEEE Transactions on Microwave Theory and Techniques*, Oct. 2009, vol. 57, n. 10, pp. 2605-2613.
- [13] "ERC Recommendations 70-03 relating to the use of short range devices (SRD)", *Eur. Postal Telecommunications Administration Conf.*, CEPT-ERC 70-03, Annex 12, Tromso, Norway, 1997.
- [14] <http://www.speag.com/measurement/liquids/>.
- [15] *ICNIRP. Guidelines for limiting exposure to time-varying electric, magnetic, and electromagnetic fields*, Health Phys., 1998, 74, pp. 494-5229.
- [16] *FCC, Evaluating Compliance with FCC Guidelines for Human Exposure to Radiofrequency Electromagnetic Fields*, Supplement C to OET Bulletin 65, Washington, D.C. 20554, Jun. 2001.
- [17] H. S. Tsai, M. J. V. Rodwell, and R. A. York, "Planar amplifier array with improved bandwidth using folded slots", *IEEE Microwave Guided Wave Lett.*, Apr. 1994, vol. 4, n. 4, pp. 112-114.
- [18] R. Carta, P. Jourand, B. Hermans, J. Thoné, D. Brosteaux, T. Vervust, F. Bossuyt, F. Axisa, J. Vanfleteren, R. Puers, "Design and Implementation of advanced systems in a flexible-stretchable technology for biomedical applications", *Sensors and Actuators*, March 2009, pp. 79-87.
- [19] J. Govaerts, W. Christiaens, E. Bosman, and J. Vanfleteren, "Fabrication Process for Embedding Thin Chips in Flat Flexible Substrate", *IEEE Transactions on Advanced Packaging*, Feb. 2009, vol. 32, n. 1, pp. 77-83.
- [20] <http://www.hirose-connectors.com>.
- [21] C. Gabriel, S. Gabriel and E. Corthout, "The dielectric properties of biological tissues: I. Literature survey", *Physics in Medicine and Biology*, 1996, vol. 41, n. 11, pp. 2231-2249.
- [22] S. Gabriel, R. W. Lau and C. Gabriel, "The dielectric properties of biological tissues: II. Measurements in the frequency range 10 Hz to 20 GHz", *Physics in Medicine and Biology*, 1996, vol. 41, n. 11, pp. 2251-2269.
- [23] C. Gabriel, S. Gabriel and E. Corthout, "The dielectric properties of biological tissues: III. Parametric models for the dielectric spectrum of tissues", *Physics in Medicine and Biology*, 1996, vol. 41, n. 11, pp. 2271-2293.
- [24] J. Kim, Y. Rahmat-Samii, "Implanted Antennas Inside a Human Body: Simulations, Design, and Characterization", *IEEE Transactions on Microwave Theory and Techniques*, Aug. 2004, vol. 52, n. 8, pp. 1934-1943.
- [25] G. Collin, A. Chami, C. Luxey, P. Le Thuc, and R. Staraj, "Small Electrical Antenna for Saw Sensor Biotelemetry", *Microwave and Optical Technology Letters*, July 2009, vol. 51, n. 10, pp. 2286-2293.
- [26] J. P. Reilly, *Applied Bioelectricity, From Electrical Stimulation to Electropathology*, New York: Springer-Verlag, 1998.
- [27] F. X. Hart, N. J. Berner, and R. L. McMillen, "Modelling the Anisotropic Electrical Properties of Skeletal Muscle", *Phys. Med. Biol.*, 1999, vol. 44, pp. 413-421.
- [28] D. Miklavčič, N. Pavšelj, F. X. Hart, "Electric Properties of Tissues", *Wiley Encyclopedia of Biomedical Engineering*, 2006.
- [29] <http://www.speag.com/measurement/dasy5/index.php>
- [30] *CENELEC EN50383, Basic standard for the calculation and measurement of electromagnetic field strength and SAR related to human exposure from radio base stations and fixed terminal stations for wireless telecommunication systems (110 MHz Ũ 40 GHz)*, Sept. 2002.
- [31] <http://www.speag.com/measurement/probes/ex3.php>
- [32] *IEEE 1528/D1.2, Recommended Practice for Determining the Spatial-Peak Specific Absorption Rate (SAR) in the Human Body Due to Wireless Communications Devices: Measurement Techniques*, 445 Hoes Lane, P.O. Box 1331, Piscataway, NJ 08855-1331, USA, Apr. 2003.